

# Phytosynthesized of Silver Nanoparticles; Antimicrobial, Antibiofilm Activities Against E.coli Pathogenic Isolated From Urinary Tract Infection

Massoumeh Mohammadizadeh

University of Kashan

Fershteh Jookar Kashi (✉ [jookar@kashanu.ac.ir](mailto:jookar@kashanu.ac.ir))

University of Kashan <https://orcid.org/0000-0002-8332-1269>

---

## Research Article

**Keywords:** Biofilms, Antimicrobials, Cytotoxicity, E.coli (all potentially pathogenic types), Bacillus

**Posted Date:** March 5th, 2021

**DOI:** <https://doi.org/10.21203/rs.3.rs-271404/v1>

**License:**  This work is licensed under a Creative Commons Attribution 4.0 International License.

[Read Full License](#)

---

## **Phytosynthesized of silver nanoparticles; antimicrobial, antibiofilm activities against *E.coli* pathogenic isolated from Urinary Tract Infection**

**Masoumeh Mohammadizadeh<sup>1</sup>, Fereshteh Jookar Kashi<sup>\*2</sup>**

<sup>1,2</sup> Department of Cell and Molecular Biology, Faculty of Chemistry, University of Kashan, Kashan 8731751167, Islamic Republic of Iran

Fereshteh Jookar Kashi

Assistant Professor of Microbiology

Department of Cell and Molecular Biology

Faculty of Chemistry, University of Kashan

Kashan, Islamic Republic of Iran

Fax: +98-03155912397

Tel: +98-3155913042

E-mail: jookar@kashanu.ac.ir

ORCID ID: 0000-0002-8332-1269

### **Abstract**

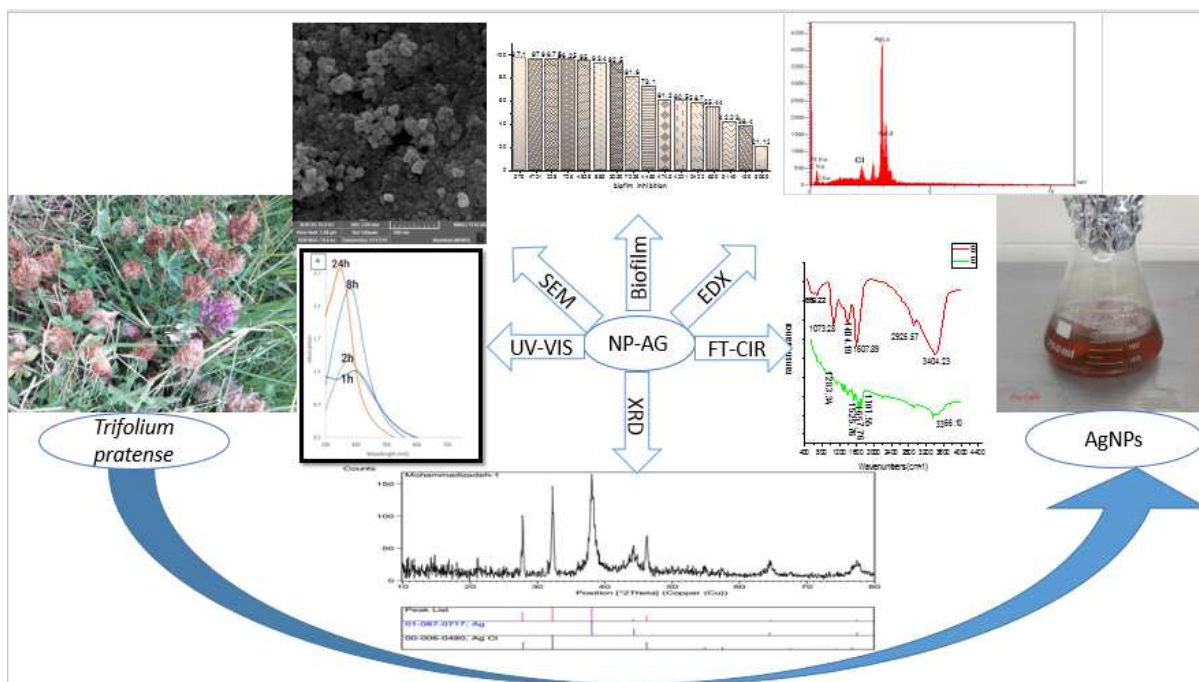
The most common cause of urinary tract infections (UTI) is uropathogenic *Escherichia coli*, which is often resistant to antibiotics. *E. coli* can form biofilms on urinary catheters. The biofilm protects *E. coli* against various factors. In this study, silver nanoparticles (AgNPS) were synthesized using *Trifolium pratense* L. extract as a reducing agent. The AgNPs were characterized by visible UV spectroscopy, a diffraction pattern (XRD), transmission electron microscopy (SEM), and energy dispersion spectroscopy (EDX). The AgNPs had a spherical shape with an average particle of 19 nm. Biological properties were also evaluated using biofilm inhibition, anticancer, antimicrobial activity. The brine shrimp lethality assay was applied to evaluate the anticancer activity of the nanoparticles. The silver nanoparticles with LC<sub>50</sub> (1.3 µg/ml) had the highest

cytotoxicity activity. The antimicrobial activity of nanoparticles was evaluated by the agar diffusion method, minimum inhibitory concentration, and minimum bactericidal concentration in the range of 1.00 to 0.0312 and 2.00 to 0.0312, respectively. The nanoparticles exhibited a high antimicrobial effect against human *E.coli* pathogenic strains isolated from Urinary Tract Infection. The effect of biofilm inhibition on antibiotic resistant clinical strains by silver nanoparticles showed that silver nanoparticles inhibited biofilm between 21.12 to 97.10%.

**Keywords:** Biofilms, Antimicrobials, Cytotoxicity, *E.coli* (all potentially pathogenic types), *Bacillus*

### **Highlights**

- Biosynthesis of novel AgNPs using *T. pretense* L.
- A new AgNPs as antimicrobial agent against urinary tract infections.
- AgNPs showed good antibiofilm effect against pathogenic *E.coli* strains
- AgNPs synthesized showed a high cytotoxicity effect.



## Introduction

Nanotechnology describes nanoscale materials (Saxena, Tripathi, Zafar, & Singh, 2012). Nanotechnology is now widely innovated in scientific fields such as new therapies, medicine, tissue engineering, diagnostic concepts, drug delivery, and gene silencing (Rajendran et al., 2015).

Catalytic, electronic, magnetic, optical, and antimicrobial properties of metal nanoparticles lead them to be used in various fields, including chemistry, energy, and medicine (Anandalakshmi, Venugobal, & Ramasamy, 2016).

The properties of nanoparticles depend on their size, morphology and distribution. Nanoparticles such as silver, gold, zinc oxide, platinum have medical and pharmaceutical applications. These nanoparticles can also be used in products such as toothpaste and cosmetics (Hashoosh, Fadhil, & Al-Ani, 2014).

Physical and chemical methods are utilized to synthesize and stabilize nanoparticles (Sharma, Yngard, & Lin, 2009). These methods include solution reduction, photochemical reactions in reverse micelles, electrochemical reduction, heat evaporation, and radiation assisting techniques. Physical and chemical methods have generally been applied

successfully in synthesizing nanomaterials in large quantities over a short period of time (Allafchian, Mirahmadi-Zare, Jalali, Hashemi, & Vahabi, 2016).

However, these methods successfully produce nanoparticles; they are harmful to human health and the environment due to hazardous and toxic chemicals (Dhand et al., 2016). An environmentally friendly and cost-effective method is used to produce nanoparticles (Behravan et al., 2019). The antimicrobial activity of silver nanoparticles is confirmed against a wide range of microorganisms. Also, recent studies showed that silver nanoparticles are antimicrobial agents. However, Sondi et al. reported the antibacterial effect of silver nanoparticles against *Escherichia coli* as a microbial model (Krishnaraj et al., 2010).

Generally, various bacteria such as *E.coli*, *Pseudomonas aeruginosa*, *Enterococcus*, *Proteus mirabilis*, *Klebsiella pneumonia* are contributed to urinary tract infections that can form biofilms on catheters. The biofilm causes them to become resistant to antibiotics, which are a threat to health. Strategies are needed to kill the antibiotic-resistant bacteria that form a biofilm (Lopez-Carrizales et al., 2018).

Plant compounds are useful for synthesizing nanoparticles because they do not require complex processes, including intracellular synthesis, purification, and microbial cell preservation (Ravichandran, Vasanthi, Shalini, Shah, & Harish, 2016).

The plants include *Solanum lycopersicums*, *Hibiscus cannabinus* stem, *Hibiscus cannabinus* leaf, *Ananas comosus*, and *Hibiscus cannabinus* leaf have been applied for green synthesis nanoparticle (Bindhu, Amala, & Jeeva, 2017). Ashuk Kumar et al. synthesized AgNPs using *Gloriosa.superba* leaf extract (Annamalai, Christina, Sudha, Kalpana, & Lakshmi, 2013). The red clover (*Trifolium pratense L.*) has a high concentration of iso-flavonoids, compounds that are widely distributed in the Leguminosae family (Dixon, 2004).

Furthermore, it has been refined in traditional medicine, which treats coughs, asthma, eczema, and eye diseases (Booth et al., 2006). GLC-MS analysis results determined twenty-five compositions from *T. pratense* leaves, flowers, and seeds (Buttery, Kamm, & Ling, 1984). The major volatile compounds were as follows leaves (3-hexenyl acetate, 3-hexenol, and  $\beta$ -okimenes), flowers (acetophenone, methyl cinnamate and 1-phenylethanol), and seed pods ( $\beta$ -okimenes, unknown) (Figueiredo, Rodrigues, & do Céu Costa, 2007).

The objective of this study is to synthesize AgNPs using *T. pratense*. Also, the biological activity of the nanoparticles was performed using anticancer, antibiofilm, and antimicrobial activity against uropathogenic *Escherichia coli* isolated from urinary tract infections. Furthermore, the silver nanoparticles were characterized by UV-Visible, XRD, FE-SEM, and EDX methods.

## **Material and Methods**

### **Collection, identification, and extraction**

*Trifolium pratense* flowers were collected in spring near Yasuj, Kohgiluyeh, and BoyerAhmad Province, Iran. The flowers are thoroughly washed with two litres of distilled water and stored at room temperature for 2 days, then split into small pieces. To prepare the aqueous extract, 10 g *T. pratense* was placed in 100 ml sterile distilled water (ratio: 1:10) for 20 min at 50 °C. The extract was isolated with Whitman filter paper and kept for further processing at 4 °C.

### **Characteristics of silver nanoparticles**

The plant extract was added to 1mM of AgNO<sub>3</sub> solution and incubated at 60 °C. Also, AgNO<sub>3</sub> solution was incubated as a control. The synthesis of silver nanoparticles was confirmed using colour change to brown. To evaluate the synthesis of Ag nanoparticles, the absorbance was measured using a Shimadzu (Model No. UV 1800) spectrophotometer in the range of 300 to 800 nm at different times.

Moreover, the Fourier-transform infrared spectroscopy (FT-IR) spectra of silver nanoparticles were measured using FTIR spectrometer (Brucker, Germany) with a KBr bullet in the range of 4000-400 cm<sup>-1</sup>. The crystalline silver nanoparticles were determined by X-ray diffraction (XRD) (Panalytical, Netherlands). Furthermore, the size of the nanoparticles was evaluated by the Debye-Scherrer formula (Ajitha, B., Reddy, Y. A. K., & Reddy, P. S. (2014)). Also, the energy dispersive X-ray (EDX) and scanning electron microscope (SEM) (Tescan, Czech) was performed to investigate the morphology and the chemical composition of the nanoparticles.

### **Antibacterial activity**

The antimicrobial effect of the nanoparticles was measured according to the protocol of Clinical and Laboratory Standard Institute (Clinical and Laboratory Standards Institute, (2020)). The antibacterial

effect of the AgNps was determined against positive and negative bacteria by the agar diffusion method.

In this study, some human pathogens include *p. aeruginosa* (ATCC27853), *K. pneumonia* (ATCC 10031), *Salmonella paratyphi-A* serotype (ATCC 5702), *Staphylococcus aureus* (AECC 29737), *Shigella dysenteriae* (PTCC 1188), *Staphylococcus epidermis* (ATCC12228), *Bacillus subtilis* (ATCC 6633), and *Escherichia coli* (ATCC 12228) were evaluated. The suspension adjusted 0.5 McFarland standard were prepared in nutrient broth at 37 °C. A 100 µl of the suspension was inoculated on Muller-Hinton agar.

Afterwards, 10 µl of the nanoparticle solution (30 mg/ml) was inserted into the well. The plates were incubated at 37 °C for 24 h. The antibacterial activity was evaluated by measuring the diameter of inhibition zones.

### **Determination of minimum inhibition concentration**

In this method, the minimum inhibition concentration (MIC) was calculated for the susceptible microorganisms to the nanoparticles. The MIC value was evaluated using the microdilution method. For this purpose, 95 µl of TSB medium, 5µl bacterial suspension adjusted 0.5 McFarland, and 100 µl of different concentrations silver nanoparticles (0.03125, 0.0625, 0.025, 0.25, 0.5). (0, 1 and 2 mg/ml) were added to each well. Furthermore, 195 µl of culture medium and 5 µl of the suspension were used as controls. The microplate was then incubated at 37 °C for 24 h. Microbial growth was characterized by the presence of turbidity at the bottom of the well.

To measure lethality, after 24 h, 5µl of each clean-well was inoculated on nutrient agar medium and incubated at 37 °C for 24 h. The concentration that did not grow after 24 h resulted in the killing of the bacteria, and the lowest concentration was considered the minimum bactericidal concentration.

### **Biofilm inhibition assay**

Sixteen human pathogenic *E.coli* strains were isolated and collected from suspected infected Urinary tract infection (UTI) patients. According to microplate biofilm assay, the antibiofilm effect of the silver nanoparticles was evaluated against *E.coli* strains.

At first, 100 µl of the nanoparticles (2mg/ml) and 100 µl of each of the diluted strains were added to each well. Moreover, 200 µl of TSB and the bacteria suspensions were negative and positive control, respectively. The microplate was incubated for 24 h at 37 °C. The 1% crystal violet was

then added to each well, and after 10 min, the crystal violet was washed with distilled water and allowed to dry. Finally, 200µl of acetic acid was added to each well, and after 15 min, the optical density (OD) was measured using ELISA at 570 nm. The following formula calculated the percentage of biofilm inhibition of the samples (Stepanović et al., 2007).

$$\text{Inhibition Percentage} = \frac{100 \times (C-B) - (T-B)}{(C-B)}$$

In this equation, C is equal to the mean biofilm absorbance, the mean absorbance of well containing the sample affected. B is the mean absorbance of the wells containing the medium (control). It was also repeated three times to ensure the test.

### **Evaluation of anticancer activity**

The cytotoxicity activity of biosynthesized AgNPs was investigated using Brine Shrimp Lethality Assay (BSLA).

*Artemia salina* eggs were grown in artificial seawater (pH 9) for 48 h. The different concentrations (0, 10, 100, 300, 500, 700, and 1000 µg) of biosynthesized Ag NPs were added to the vial, including 5 ml seawater and ten brine shrimp larvae, and incubated at 25 °C for 24h. Brine shrimp death was observed at regular intervals. Vincristine sulfate (VS) was applied as a positive control. These tests were repeated three times. The lethality percentage was recorded according to formula (Arulvasu, C., Jennifer, S. M., Prabhu, D., & Chandhirasekar, D. (2014)).

$$\text{Lethality percentage} = [(m-M)/s] \times 100$$

m: Average number of dead larvae sampled

M: Average number of dead larvae control

s: Average number of live larvae control

### **Results and discussion**

#### **Characterization of nanoparticles**

The formation of extracellular was observed with a change color from yellowish to deep brown due to the excitation of the localized surface plasmon vibrations of the nanoparticles.

The changing color from yellowish to brown confirmed the synthesis of the nanoparticles.

One of the properties of metal nanoparticles is their optical properties, which change (Mohamed, M. B., Volkov, V., Link, S., & El-

Sayed, M. A. (2000)). The color change indicated the biosynthesis of silver nanoparticles using aqueous extract of *T. pretense* (Fig. 1).

Free electrons in silver nanoparticles are excited by visible light absorption and transmitted to higher energy levels. The electrons are unstable and return to their original energy levels and emit a photon simultaneously (Thangaraju, Venkatalakshmi, Chinnasamy, & Kannaiyan, 2012).

Figure 1 shows the maximum wavelength of about (450 nm), similar to other researchers (Singh, Bhardwaj, Dubey, & Prabhune, 2015). The optimal conditions for the preparation of these nanoparticles were 1mM of silver nitrate, 5 ml of aqueous extract, at 65 °C for 24 h. The effect of contact time (0, 2, 8, 12, 24h) on the formation of nanoparticles was investigated under constant conditions.

As exhibited in figure 1, with the increased time, an increasing trend in absorbance was exhibited.

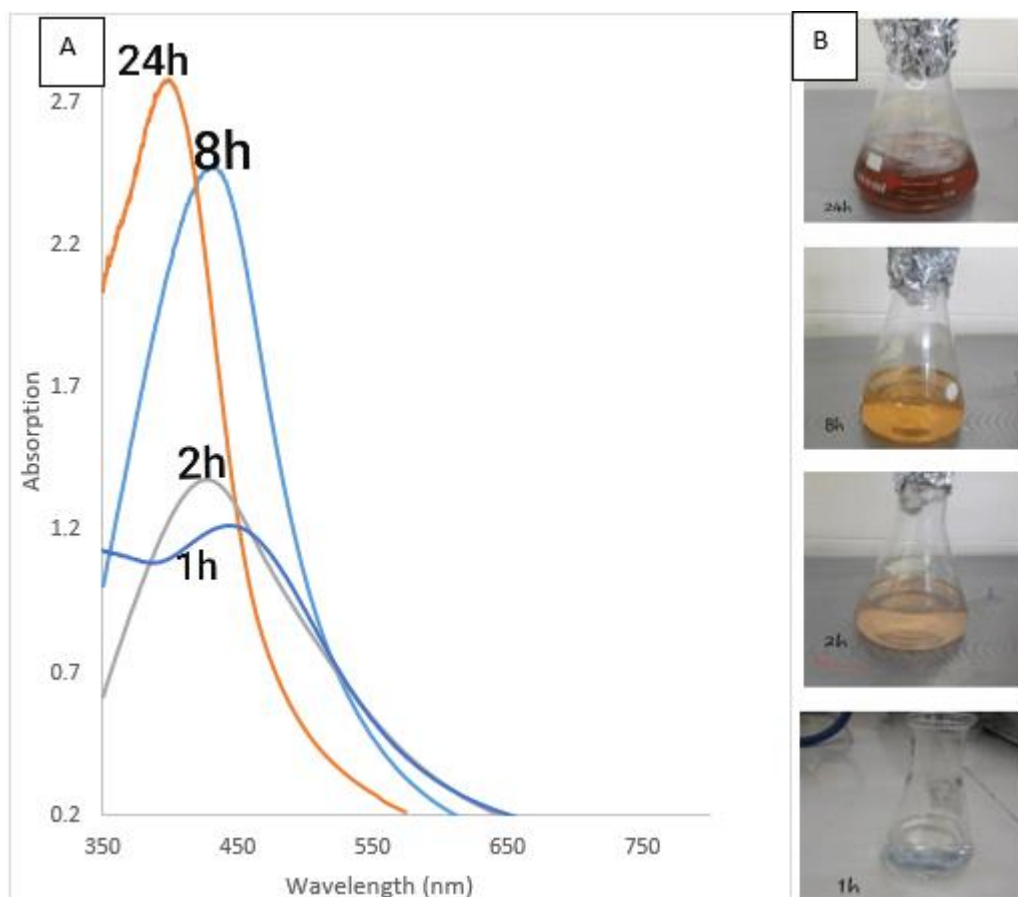


Figure 1. Spectrophotometric analysis (A) and visible observation (B) of biosynthesis of AgNps over time.

## FTIR

Comparing the spectral pattern of silver nanoparticles and the extract showed that nanoparticles contain compounds in the extract. They are usually formed as a layer around the nanoparticles and can play a role in the stability of nanoparticles. The results showed that peaks in regions  $3404\text{ cm}^{-1}$  determined OH bond in phenols and alcohols. Moreover, the absorption band indicated in region  $2925\text{ cm}^{-1}$  corresponds to CH stretching vibration in alkyls (methylene group), and  $1607\text{ cm}^{-1}$  corresponding to NH bonds in first amines. Furthermore, the band at  $1404\text{ cm}^{-1}$  corresponding OH stretching indicates that phenols. Whereas the absorption band determined in region  $1073\text{ cm}^{-1}$  correspond to the CO stretching in the first alcohols. Phenolic compounds present in the plant are among the major contributors to reducing silver ions and the synthesis of nanoparticles.

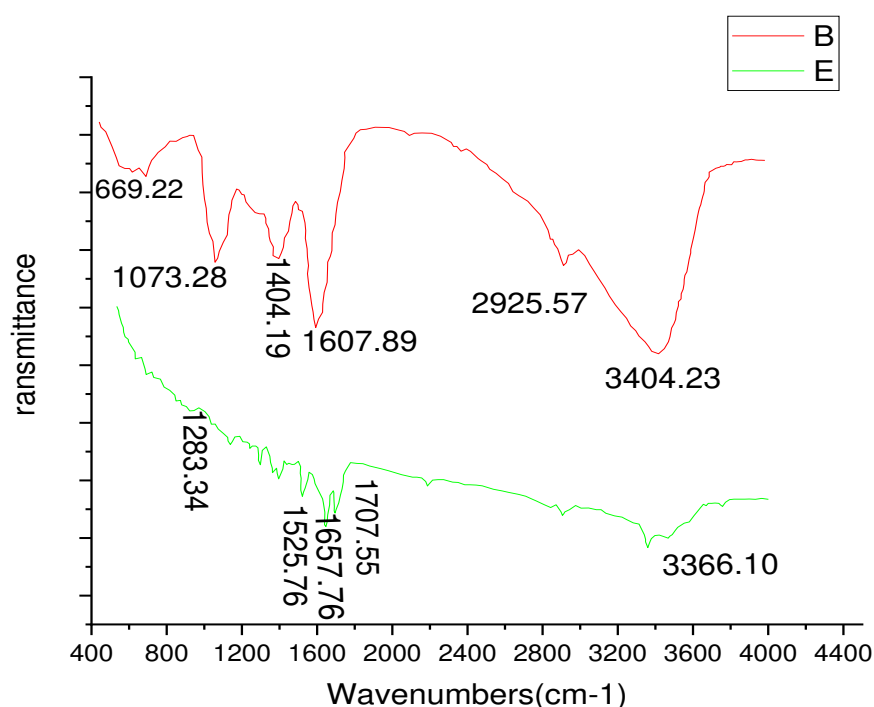


Figure 2. FT-IR spectra of the extract (B) and the silver nanoparticles synthesized from the extract (E)

## SEM analysis

The surface morphology and structure of the synthesized silver nanoparticles were characterized using SEM. Figure 4 exhibited that the silver nanoparticle was an almost spherical shape with a range between

19 to 46 nm and an average size of 34.42 nm. The results of the size distribution analysis of silver nanoparticles are shown in (Figure. 3).

### **EDX**

The EDX result confirmed the present silver as a major element. Moreover, the present O, C, and N were determined in the EDX spectrum (Figure 3). The presence of biomaterial is one of the advantages of nanoparticles synthesized using plant extracts compared to chemical methods.

Similar results also reported the formation of silver nanoparticles performed using *Artemisia nilagirica* leaf and *Artocarpus heterophyllus* seed extract (Anandalakshmi, K., Venugobal, J., & Ramasamy, V. (2016)).

### **XRD**

X-ray diffraction is used to study the structure of crystalline materials. The spectral region results can obtain information on the structure, material, and quantities of the elements (Cullity & Stock, 2001). X-ray diffraction analysis was used to investigate and study the synthesized silver nanoparticles (Figure 3).

The average size of crystal was calculated by calculating the width of peaks formed in the samples using the Debay-Scherer formula: (Ajitha, B., Reddy, Y. A. K., & Reddy, P. S. (2014))

$$D = (0.9\lambda / \beta \cos\Theta).$$

Where  $\beta$  is the width of the peaks at half the maximum height,  $\lambda$  is the X-ray wavelength equal to 54.1 nm. Moreover,  $\Theta$  is the angle between the reflected beam and the radiation, and D is the crystal size. As shown in the figure, clear peaks in the areas  $2\Theta = 27.82, 32.25, 38.07, 44.25, 46.25, 64, 57, \text{ and } 77.3$  are the reason for the successful synthesis of nanoparticles. The presence of sharp peaks in the patterns indicates a high degree of crystallinity for the nanoparticles. The average size of the synthesized crystal was estimated at 22.25 nm, completely consistent with SEM results.

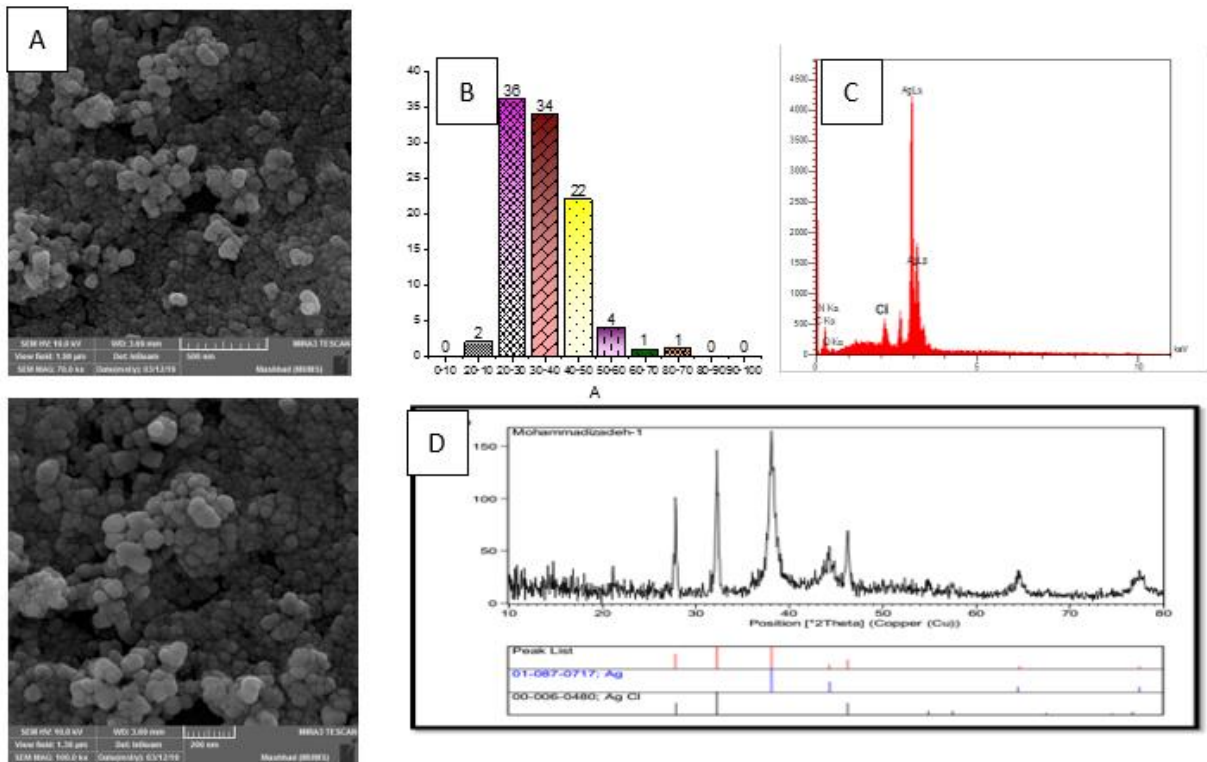


Figure 3. SEM images of the silver nanoparticles synthesized from the extract (A). Frequency distribution of the size of silver nanoparticles synthesized from the extract (B). X-ray diffraction energy spectra for the silver nanoparticles synthesized from the extract (C). XRD spectra of the silver nanoparticles synthesized from the extract (D).

## Antimicrobial activity

The antimicrobial effect of the silver nanoparticles, the extract and composite of extract and silver nanoparticles were measured by the present or absent zone of the inhibition, and the results are shown in Table 1.

Table 1. Antimicrobial activity of silver nanoparticles and the plant extract.

Bacterial strains	Silver nanoparticles	Composite nanoparticles	Extracts
	Inhibition zones (mm)		
<i>B. subtilis</i>	9	9	-
<i>S. epidermidis</i>	9	7	-
<i>S. aureus</i>	7	-	-
<i>E. coli</i>	-	-	-
<i>K. pneumonia</i>	-	-	-
<i>S. paratyphi A serotype</i>	10	-	-
<i>P. aeruginosa</i>	10	-	-
<i>S. dysenteriae</i>	-	-	-
<i>C. albicans</i>	-	-	-

A dash (-) determine no antimicrobial effect.

The results showed that the nanoparticles had an antimicrobial effect. In contrast, the extract shows no antimicrobial activity.

The nanoparticles showed a zone of inhibition against *B. subtilis*, *S. epidermidis* and *P. aeruginosa* (9 mm). Moreover, *S. paratyphi A serotype* and exhibited the inhibition zone (10 mm), and the zone of *S. aureus* was 7 mm.

The composite of extract and silver nanoparticles has no antimicrobial effect except for two strains: *B. subtilis* (9 mm) and *S. epidermidis* (7 mm).

Allafchian et al. reported the antibacterial effect of silver nanoparticles against Gram-positive (*S. aureus* and *B. cereus*) and Gram-negative (*S. typhimurium* and *E. coli*) bacteria using the agar well diffusion. These nanoparticles were synthesized by *Phlomis cancellata* Bunge leaf extract. Their results proved to be almost parallel with our findings (Allafchian, Mirahmadi-Zare, Jalali, Hashemi, & Vahabi, 2016).

Furthermore, in the study by Hashoosh et al., silver nanoparticles synthesized by Aloe vera plant and Aloe vera extract had different antibacterial effects against Gram-negative bacteria (*E. coli*) and Gram-positive bacteria (*S. aureus*). The results showed that the aqueous extract of Aloe vera had no inhibitory effect. In contrast, silver nanoparticles had an inhibitory effect against *E. coli* and *S. aureus* (Hashoosh, Fadhil, & Al-Ani, 2014).

Nazar Ul Islam et al. reported synthesized silver nanoparticles using *Prunus armeniaca*. They investigated the antimicrobial properties of the nanoparticles, and the extract against *S. aureus*, *E. coli*, *P. aeruginosa* with the diameter of inhibition zone 18, 10.2 and 11.2 mm, respectively. However, the plant extract alone did not have antimicrobial activity (Islam, Amin, Shahid, & Amin, 2016). In another study by S. Yallappa et al., copper nanoparticles synthesized using aqueous extract of *Terminalia arjuna* tree bark showed good antimicrobial activity against *S. aureus*, *E. coli*, *S. typhi* and *P. aeruginosa* (Khedkar, Michael, & Khan, 2019).

## **Biofilm Inhibition**

The antibacterial effect of the silver nanoparticles was evaluated against sixteen *E. coli* strains isolated from patients with urinary tract infections. The results show that the MIC and MBC of silver nanoparticles range from 1.00 to 0.0312 and 2.00 to 0.0312, respectively (Table 2).

The biofilm formation ability was measured for each assay as a control. The percentage of biofilm inhibition of the silver nanoparticles was between 21.12 to 97.10%. The nanoparticles exhibited high ability antibiofilm against *E. coli* 579, *E. coli* 4701, *E. coli* 228, *E. coli* 726, *E. coli* 4828, *E. coli* 885, and *E. coli* 3059. Furthermore, the lowest ability antibiofilm was against *E. coli* 5149.

Biofilm inhibitory activity of nanoparticles synthesized from *Cordia. Dichotoma* was evaluated. The results showed that silver nanoparticles (100 µg/ml) inhibited *S.aureus* and *E.coli* biofilm (92% and 95%) after 12h (Bharathi, D., Vasantharaj, S., & Bhuvaneshwari, V. (2018)).

Morones-Amirez et al. reported that AgNPs inhibited biofilm activity approximately 20% (Gurunathan, Han, Kwon, & Kim, 2014).

Table .2. Results of MIC and MBC (mg /ml), and biofilm formation ability.

No.	Bacteria	Code	MIC mg /ml	MBC mg /ml	Biofilm formation power	Biofilm inhibition%	No.	Bacteria	Code	MIC mg /ml	MBC mg /ml	Biofilm formation power	Biofil m inhibit ion%
1	<i>E. coli</i>	4221	0.25	0.50	Medium	60.5	9	<i>E. coli</i>	726	0.0312	0.0625	Strong	96.25
2	<i>E. coli</i>	3059	0.0625	0.25	Strong	92.5	10	<i>E. coli</i>	228	0.0312	0.0312	Strong	96.7
3	<i>E. coli</i>	7026	0.0625	0.0625	Strong	81.6	11	<i>E. coli</i>	579	0.0312	0.0625	Strong	97.1
4	<i>E. coli</i>	159	0.50	1.00	Weak	38.4	12	<i>E. coli</i>	5149	0.50	0.50	Weak	42.23
5	<i>E. coli</i>	4701	0.0312	0.0312	Strong	97	13	<i>E. coli</i>	885	0.0312	0.0312	Strong	93.4
6	<i>E. coli</i>	4469	0.25	0.25	Medium	73.1	14	<i>E. coli</i>	3069	1.00	2.00	Weak	21.12
7	<i>E. coli</i>	2422	0.25	1.00	Medium	58.7	15	<i>E. coli</i>	659	0.25	0.25	Medium	55.44
8	<i>E. coli</i>	4745	0.25	0.25	Medium	61.2	16	<i>E. coli</i>	4828	0.0625	0.25	Strong	95

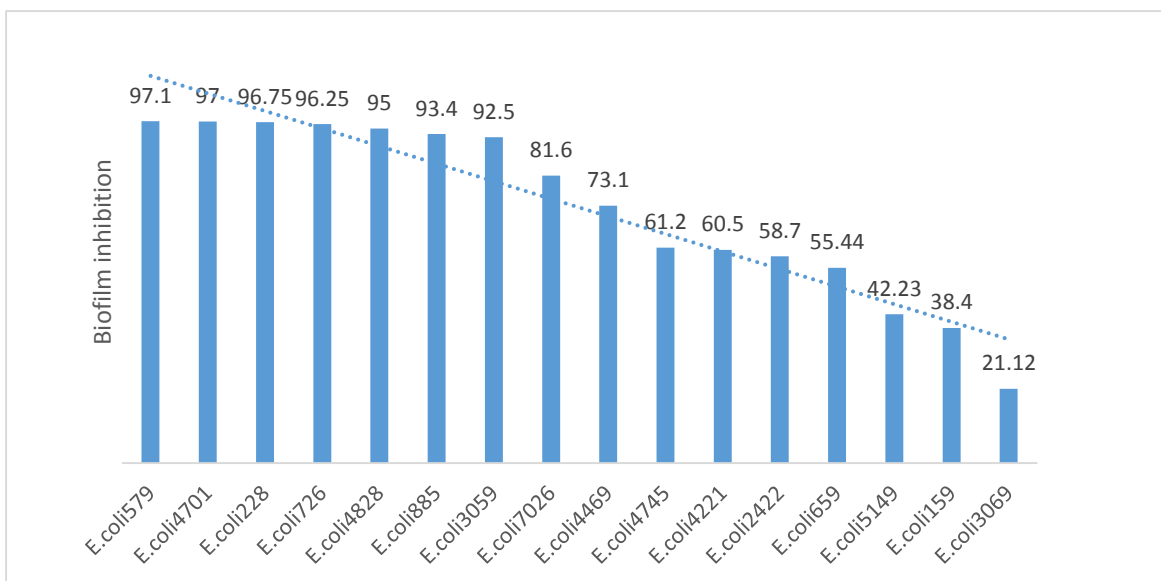


Figure 4. Biofilm inhibition percentage of the silver nanoparticles against *E.coli* clinical strains.

### Cytotoxicity

The anticancer activity of the silver nanoparticles and the percentage of dead larvae were determined at different concentrations ( $\mu\text{g/ml}$ ).

The previous study determined that  $\text{LC}_{50}$  (0.5-1 mg/ml) was weak the toxicity against *A. salina*. Moreover, The  $\text{LC}_{50}$  between 0 and 0.1 mg/ml exhibited high toxicity and 0.1-0.5 mg/ml moderate cytotoxicity. Additionally,  $\text{LC}_{50}$  above 1 mg/ml indicated the lack of toxicity against *A. salina*. (Wiji Prasetyaningrum, P., Bahtiar, A., & Hayun, H. 2018).

Our study showed that the silver nanoparticles with  $\text{LC}_{50}$  1.3  $\mu\text{g/ml}$  had high cytotoxicity and anticancer properties. Furthermore, the  $\text{LC}_{50}$  of vincristine sulfate was 0.751  $\mu\text{g/ml}$  as a positive control. Based on these results, *T. pratense* L. extract showed high cytotoxicity (Figure.5).

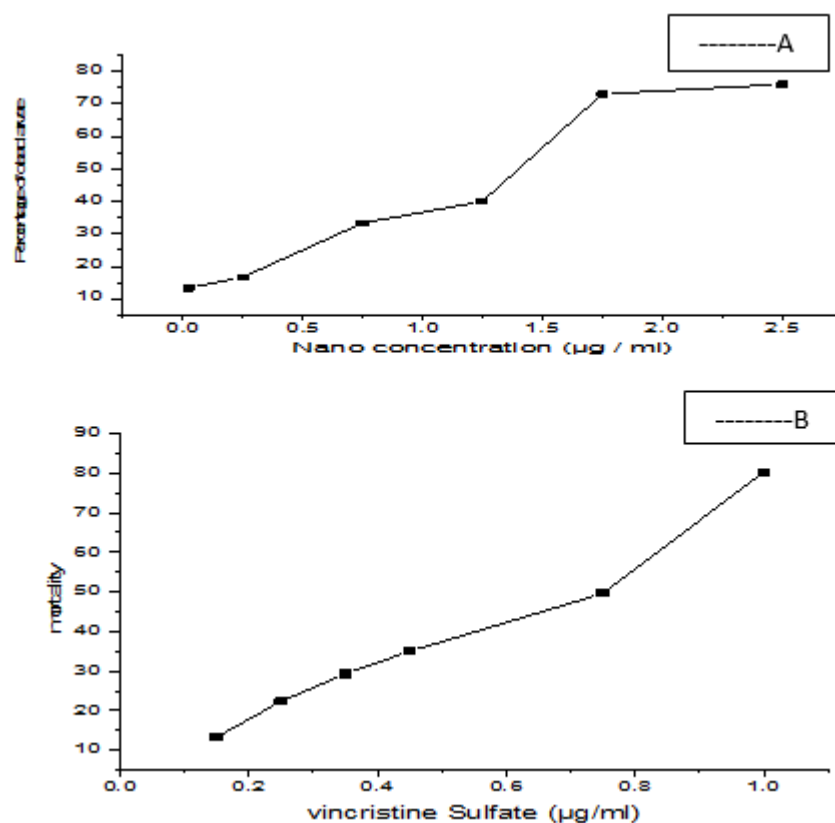


Figure 5. Cytotoxicity effect at different concentrations of the silver nanoparticles (A) and vincristine sulfate (B).

## Conclusion

For the first time in the present study, silver nanoparticles were synthesized using the *T. pratense*. The antimicrobial and antibiofilm activity of the nanoparticles were determined. Additionally, the formation of silver nanoparticles was confirmed using UV-Vis, XRD, SEM, EDX, and FTIR. However, it can be concluded that this study reports a novel, rapid, economical, and environmentally friendly procedure for the production of silver nanoparticles.

Based on results, the nanoparticles have anticancer, antimicrobial, and antibiofilm activity against UTI. Silver nanoparticles may play a role in neutralizing cell adhesives, thus preventing biofilm formation. Bacterial biofilm is highly resistant to antibiotics. Therefore, silver nanoparticles may play a major role in biofilm formation on urinary catheters.

## References

- 1) Asharani, P. V., Wu, Y. L., Gong, Z., & Valiyaveetil, S. (2008). Toxicity of silver nanoparticles in zebrafish models. *Nanotechnology*, 19(25), 255102.
- 2) Allafchian, A., Mirahmadi-Zare, S., Jalali, S., Hashemi, S., & Vahabi, M. (2016). Green synthesis of silver nanoparticles using phlomis leaf extract and

- investigation of their antibacterial activity. *Journal of Nanostructure in Chemistry*, 6(2), 129-135.
- 3) Ajitha, B., Reddy, Y. A. K., & Reddy, P. S. (2014). Biogenic nano-scale silver particles by *Tephrosia purpurea* leaf extract and their inborn antimicrobial activity. *Spectrochimica Acta Part A: Molecular and Biomolecular Spectroscopy*, 121, 164-172.
  - 4) Arulvasu, C., Jennifer, S. M., Prabhu, D., & Chandhirasekar, D. (2014). Toxicity effect of silver nanoparticles in brine shrimp *Artemia*. *The Scientific World Journal*, 2014.
  - 5) Anandalakshmi, K., Venugobal, J., & Ramasamy, V. (2016). Characterization of silver nanoparticles by green synthesis method using *Petalium murex* leaf extract and their antibacterial activity. *Applied Nanoscience*, 6(3), 399-408.
  - 6) Annamalai, A., Christina, V., Sudha, D., Kalpana, M., & Lakshmi, P. (2013). Green synthesis, characterization and antimicrobial activity of Au NPs using *Euphorbia hirta* L. leaf extract. *Colloids and Surfaces B: Biointerfaces*, 108, 60-65.
  - 7) Bharathi, D., Vasantharaj, S., & Bhuvaneshwari, V. (2018). Green synthesis of silver nanoparticles using *Cordia dichotoma* fruit extract and its enhanced antibacterial, anti-biofilm and photo catalytic activity. *Materials Research Express*, 5(5), 055404.
  - 8) Brad, K., Zhang, Y., & Gao, J. (2017). Extraction and purification of formononetin from *Trifolium pratense* L: Physicochemical properties of its complex with lecithin. *Tropical Journal of Pharmaceutical Research*, 16(8), 1757-1763.
  - 9) Behravan, M., Panahi, A. H., Naghizadeh, A., Ziaee, M., Mahdavi, R., & Mirzapour, A. (2019). Facile green synthesis of silver nanoparticles using *Berberis vulgaris* leaf and root aqueous extract and its antibacterial activity. *International journal of biological macromolecules*, 124, 148-154.
  - 10) Bindhu, M., Amala, B. M., & Jeeva, M. (2017). Green Synthesis Of Silver Nanoparticles And Its Antibacterial Activity.
  - 11) Booth, N. L., Overk, C. R., Yao, P., Totura, S., Deng, Y., Hedayat, A., . . . Farnsworth, N. R. (2006). Seasonal variation of red clover (*Trifolium pratense* L., Fabaceae) isoflavones and estrogenic activity. *Journal of agricultural and food chemistry*, 54(4), 1277-1282.
  - 12) Buttery, R. G., Kamm, J. A., & Ling, L. C. (1984). Volatile components of red clover leaves, flowers, and seed pods: possible insect attractants. *Journal of agricultural and food chemistry*, 32(2), 254-256.
  - 13) Wayne, PA: Clinical and Laboratory Standards Institute, (2020)). (CLSI. Performance standards for antimicrobial susceptibility testing. thirtieth ed. CLSI supplement M100.
  - 14) Cullity, B. D., & Stock, S. R. (2001). *Elements of X-ray Diffraction* (Vol. 3): Prentice hall New Jersey.
  - 15) Dhand, V., Soumya, L., Bharadwaj, S., Chakra, S., Bhatt, D., & Sreedhar, B. (2016). Green synthesis of silver nanoparticles using *Coffea arabica* seed extract and its antibacterial activity. *Materials Science and Engineering: C*, 58, 36-43.
  - 16) Dixon, R. A. (2004). Phytoestrogens. *Annual review of plant biology*, 55.
  - 17) Feng, Q. L., Wu, J., Chen, G., Cui, F., Kim, T., & Kim, J. (2000). A mechanistic study of the antibacterial effect of silver ions on *Escherichia coli* and *Staphylococcus aureus*. *Journal of biomedical materials research*, 52(4), 662-668.

- 18) Figueiredo, R., Rodrigues, A. I., & do Céu Costa, M. (2007). Volatile composition of red clover (*Trifolium pratense* L.) forages in Portugal: The influence of ripening stage and ensilage. *Food chemistry*, 104(4), 1445-1453.
- 19) Gurunathan, S., Han, J. W., Kwon, D.-N., & Kim, J.-H. (2014). Enhanced antibacterial and anti-biofilm activities of silver nanoparticles against Gram-negative and Gram-positive bacteria. *Nanoscale research letters*, 9(1), 373.
- 20) Hashoosh, S. I., Fadhil, A. M., & Al-Ani, N. K. (2014). Production of Ag nanoparticles using Aloe vera extract and its antimicrobial activity. *Al-Nahrain Journal of Science*, 17(2), 165-171.
- 21) Islam, N. U., Amin, R., Shahid, M., & Amin, M. (2016). Gummy gold and silver nanoparticles of apricot (*Prunus armeniaca*) confer high stability and biological activity. *Arabian Journal of Chemistry*.
- 22) Kumar, V. S., Nagaraja, B. M., Shashikala, V., Padmasri, A. H., Madhavendra, S. S., Raju, B. D., & Rao, K. R. (2004). Highly efficient Ag/C catalyst prepared by electro-chemical deposition method in controlling microorganisms in water. *Journal of Molecular Catalysis A: Chemical*, 223(1-2), 313-319.
- 23) Khedkar, M., Michael, P. E., & Khan, S. R. (2019). Copper and Copper Oxide Nanoparticles: Applications in Catalysis.
- 24) Krishnaraj, C., Jagan, E., Rajasekar, S., Selvakumar, P., Kalaichelvan, P., & Mohan, N. (2010). Synthesis of silver nanoparticles using *Acalypha indica* leaf extracts and its antibacterial activity against water borne pathogens. *Colloids and Surfaces B: Biointerfaces*, 76(1), 50-56.
- 25) Lopez-Carrizales, M., Velasco, K. I., Castillo, C., Flores, A., Magaña, M., Martinez-Castanon, G. A., & Martinez-Gutierrez, F. (2018). In vitro synergism of silver nanoparticles with antibiotics as an alternative treatment in multiresistant uropathogens. *Antibiotics*, 7(2), 50.
- 26) Luo, J., Chan, W. B., Wang, L., & Zhong, C. J. (2010). Probing interfacial interactions of bacteria on metal nanoparticles and substrates with different surface properties. *International journal of antimicrobial agents*, 36(6), 549-556.
- 27) Masurkar, S. A., Chaudhari, P. R., Shidore, V. B., & Kamble, S. P. (2012). Effect of biologically synthesised silver nanoparticles on *Staphylococcus aureus* biofilm quenching and prevention of biofilm formation. *IET nanobiotechnology*, 6(3), 110-114.
- 28) Mohanpuria, P., Rana, N. K., & Yadav, S. K. (2008). Biosynthesis of nanoparticles: technological concepts and future applications. *Journal of nanoparticle research*, 10(3), 507-517.
- 29) Mohamed, M. B., Volkov, V., Link, S., & El-Sayed, M. A. (2000). The lightning'gold nanorods: fluorescence enhancement of over a million compared to the gold metal. *Chemical Physics Letters*, 317(6), 517-523.
- 30) Patra, J. K., & Baek, K.-H. (2017). Antibacterial activity and synergistic antibacterial potential of biosynthesized silver nanoparticles against foodborne pathogenic bacteria along with its anticandidal and antioxidant effects. *Frontiers in microbiology*, 8, 167.
- 31) Rajendran, R., Ganesan, N., Balu, S. K., Alagar, S., Thandavamoorthy, P., & Thiruvengadam, D. (2015). Green synthesis, characterization, antimicrobial and cytotoxic effects of silver nanoparticles using *Origanum heracleoticum* L. Leaf extract. *Int. J. Pharm. Pharm. Sci*, 7(4), 288-293.
- 32) Ravichandran, V., Vasanthi, S., Shalini, S., Shah, S. A. A., & Harish, R. (2016). Green synthesis of silver nanoparticles using *Atrocarpus altilis* leaf extract and

- the study of their antimicrobial and antioxidant activity. *Materials Letters*, 180, 264-267.
- 33) Saxena, A., Tripathi, R., Zafar, F., & Singh, P. (2012). Green synthesis of silver nanoparticles using aqueous solution of *Ficus benghalensis* leaf extract and characterization of their antibacterial activity. *Materials Letters*, 67(1), 91-94.
  - 34) Sharma, V. K., Yngard, R. A., & Lin, Y. (2009). Silver nanoparticles: green synthesis and their antimicrobial activities. *Advances in colloid and interface science*, 145(1-2), 83-96.
  - 35) Singh, P. K., Bhardwaj, K., Dubey, P., & Prabhune, A. (2015). UV-assisted size sampling and antibacterial screening of *Lantana camara* leaf extract synthesized silver nanoparticles. *RSC Advances*, 5(31), 24513-24520.
  - 36) Sondi, I., & Salopek-Sondi, B. (2004). Silver nanoparticles as antimicrobial agent: a case study on *E. coli* as a model for Gram-negative bacteria. *Journal of colloid and interface science*, 275(1), 177-182.
  - 37) Stepanović, S., Vuković, D., Hola, V., BONAVENTURA, G. D., Djukić, S., Ćirković, I., & Ruzicka, F. (2007). Quantification of biofilm in microtiter plates: overview of testing conditions and practical recommendations for assessment of biofilm production by staphylococci. *Apmis*, 115(8), 891-899.
  - 38) Thangaraju, N., Venkatalakshmi, R., Chinnasamy, A., & Kannaiyan, P. (2012). Synthesis of silver nanoparticles and the antibacterial and anticancer activities of the crude extract of *Sargassum polycystum* C. *Agardh. Nano Biomed Eng*, 4(2), 89-94.
  - 39) Vaidyanathan, R., Gopalram, S., Kalishwaralal, K., Deepak, V., Pandian, S. R. K., & Gurunathan, S. (2010). Enhanced silver nanoparticle synthesis by optimization of nitrate reductase activity. *Colloids and Surfaces B: Biointerfaces*, 75(1), 335-341.
  - 40) Wiji Prasetyaningrum, P., Bahtiar, A., & Hayun, H. (2018). Synthesis and cytotoxicity evaluation of novel asymmetrical mono-carbonyl analogs of curcumin (AMACs) against Vero, HeLa, and MCF7 Cell Lines. *Scientia Pharmaceutica*, 86(2), 25.



# Figures

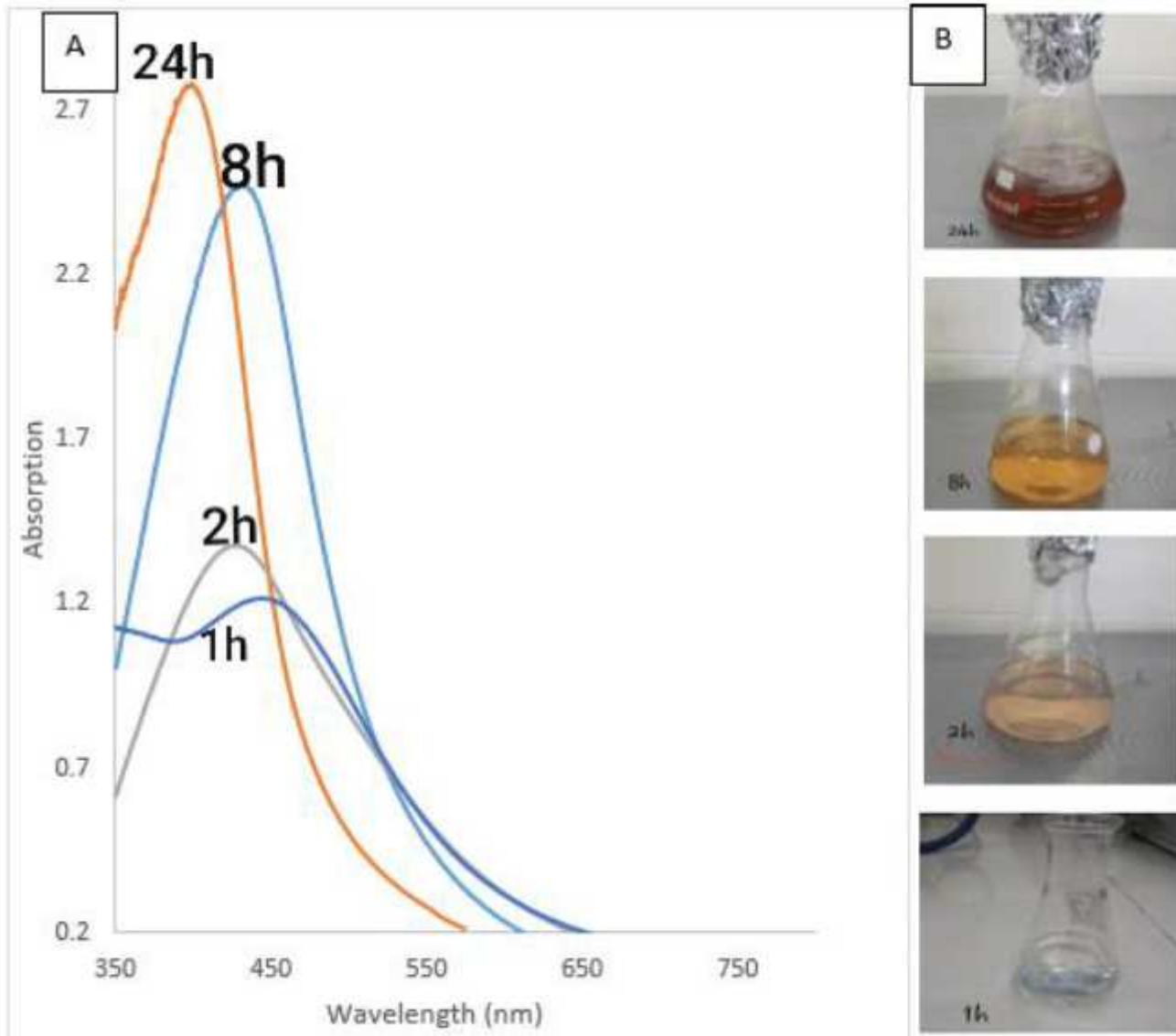


**Figure 1**

Spectrophotometric analysis (A) and visible observation (B) of biosynthesis of AgNps over time.

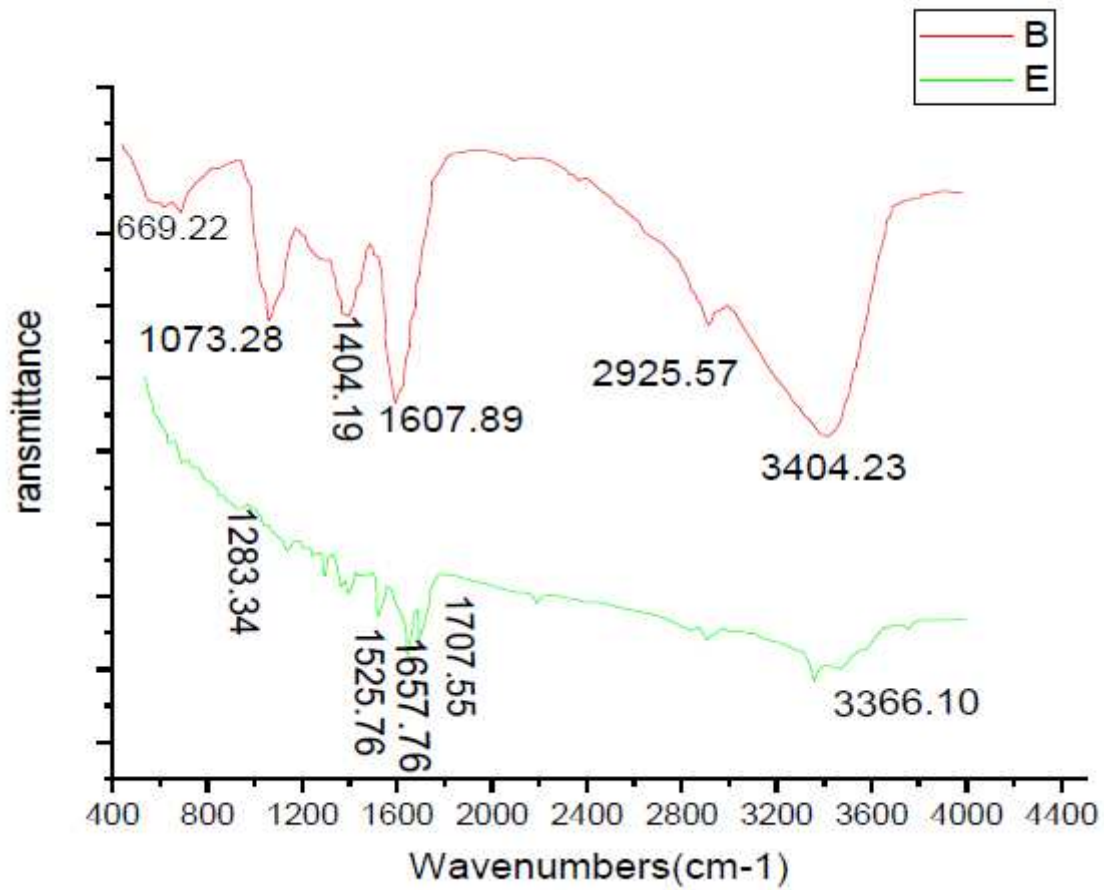
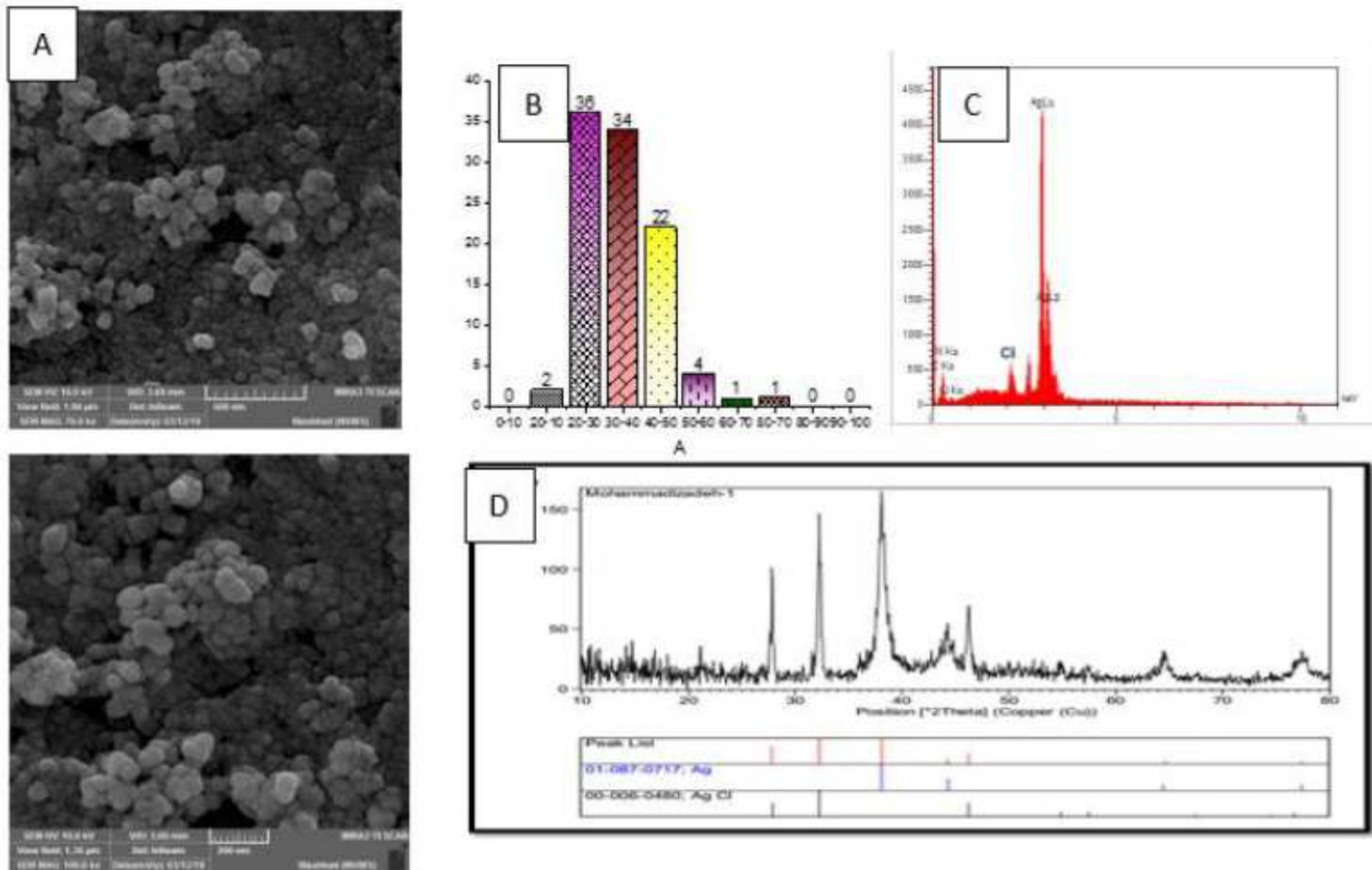


Figure 2

FT-IR spectra of the extract (B) and the silver nanoparticles synthesized from the extract (E)



**Figure 3**

SEM images of the silver nanoparticles synthesized from the extract (A). Frequency distribution of the size of silver nanoparticles synthesized from the extract (B). X-ray diffraction energy spectra for the silver nanoparticles synthesized from the extract (C). XRD spectra of the silver nanoparticles synthesized from the extract (D).

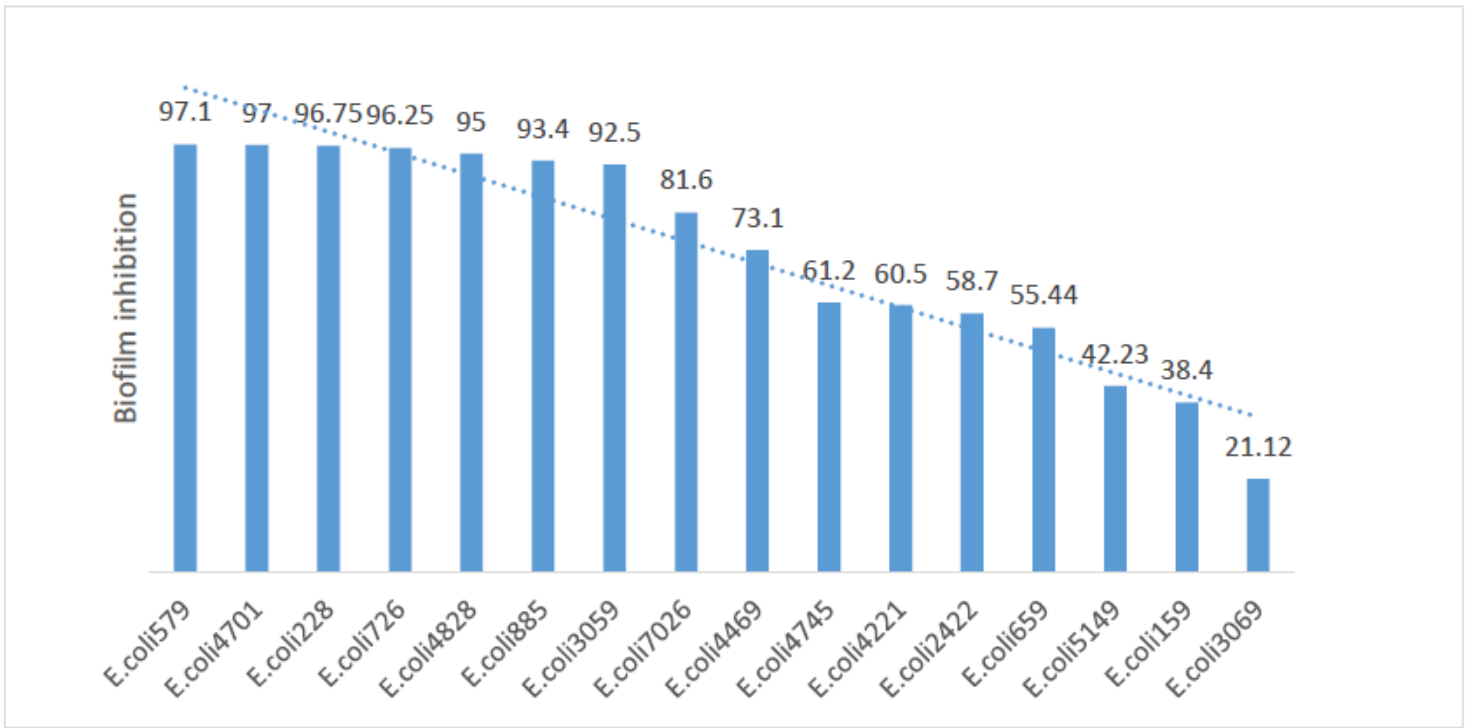


**Figure 4**

Biofilm inhibition percentage of the silver nanoparticles against E.coli clinical strains.

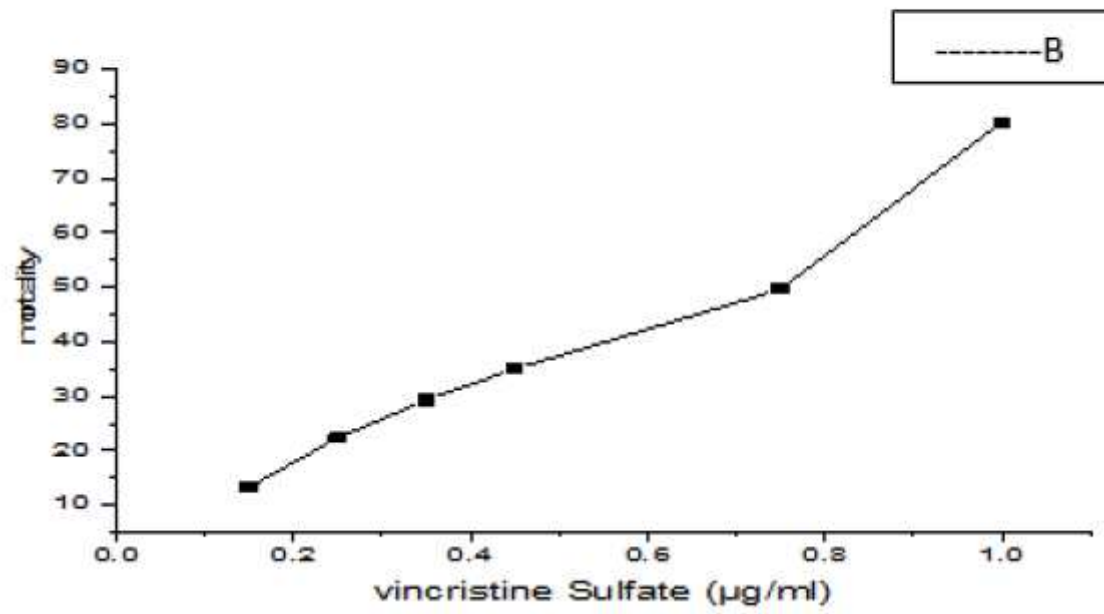
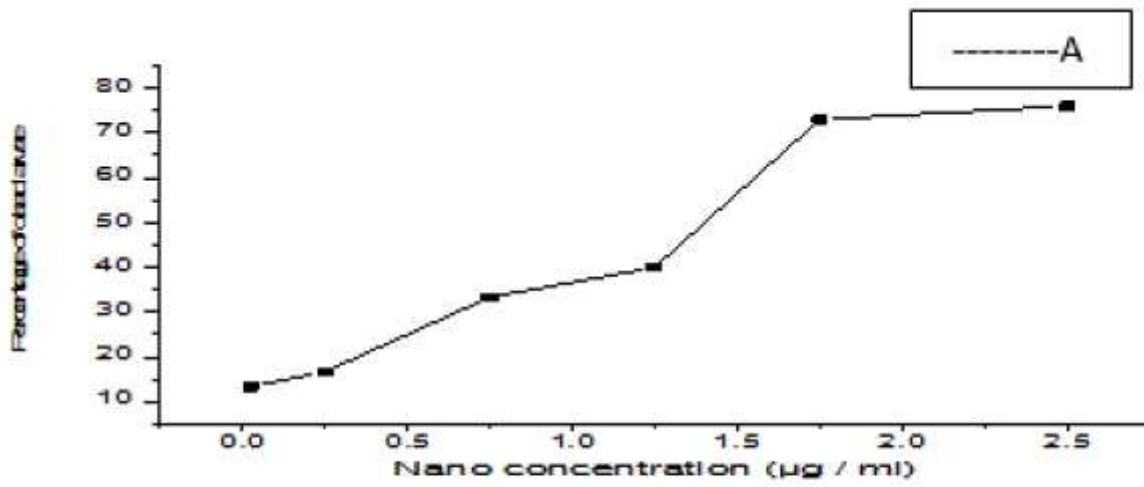


**Figure 5**  
Cytotoxicity effect at different concentrations of the silver nanoparticles (A) and vincristine sulfate (B).